RSC Advances

ROYAL SOCIETY OF CHEMISTRY

www.rsc.org/advances

RSC Advances

RSCPublishing

ARTICLE

Porphyrinated Polyimide Honeycomb Films with High Thermal Stability for HCl Gas Sensing

Cite this: DOI: 10.1039/x0xx00000x

Fu-Wen Lin,[b] Xiao-Ling Xu,[b] Ling-Shu Wan,*[a,c] Jian Wu,*[b] and Zhi-Kang Xu*[a,c]

Received 00th January 2012,
Accepted 00th January 2012

DOI: 10.1039/x0xx00000x

www.rsc.org/

We report thermally stable films with ordered pores from porphyrinated polyimides (PPIs) for HCl gas sensing. PPIs were synthesized by copolymerizing porphyrin units into the polyimide backbone. Thermal analyses reveal that the glass transition temperature and the thermal stability of PPIs are similar to that of the homopolyimide (HPI) without porphyrin units. The PPIs also show typical fluorescence emission behavior of the porphyrin units. Honeycomb films were prepared from PPIs and HPI via the breath figure method. The porous films show decreased pore diameters and change from monolayer to multilayer structure with the incorporation of porphyrin units. These are due to the interaction of porphyrin units with water molecules, as demonstrated by theoretical calculations based on density functional theory (DFT). The well-ordered porous PPI films have outstanding thermal stability. Furthermore, the films treated at different temperatures show remarkable fluorescence quenching behavior toward HCl gas with quenching ratios higher than 72%, whereas it is only about 50% for the corresponding dense film. Moreover, recovery experiments by ammonia gas demonstrate excellent reusability of the films. The PPI honeycomb films provide new opportunities in chemical sensing at high temperature.

Introduction

Chemical sensing materials have received great attention as the sensors are characterized by non-invasive measurement, easy to handle, and viability in harsh environment.[1] Among them, fluorescent sensing materials have been used for chemical sensing very early for the advantages of short response time, excellent sensitivity, and instrumental simplicity.[2] Normally, the efficiency of fluorescent sensing materials is largely dependent on the specific surface area which benefits the diffusion of analytes. As a result, porous structures are commonly designed for fluorescent sensing materials to provide high specific surface area.[3,4] The porous structures can be prepared by various methods, such as templating, lithography, emulsion, and phase separation.[5-7] The breath figure method is a fast, convenient and cost-efficient technique to fabricate highly ordered porous films.[8-13] In the breath figure process, ordered hexagonal arrays of water droplets are induced by solvent evaporative cooling and act as sacrificial templates for spherical pores to form a honeycomb-patterned porous film after further evaporation of the solvent and water.[8-23]

Functional honeycomb films were investigated for chemical sensing, and the improved sensing properties were demonstrated.[24-27] As an example, Sun *et al.*[26] prepared a pyrene/polystyrene honeycomb film by the breath figure method for nitroaromatic explosives detection, and the film shows sensitive and rapid response to 4-nitrotoluene. In this case, pyrene was blended with polystyrene and used as fluorescent molecule for chemical sensing. It is well known that porphyrin is another kind of fluorescent molecule, which can be easily incorporated into various polymers for film fabrication. Therefore, porphyrinated materials have found increasing applications in many fields including light-emitting, photodynamic therapy, and chemical sensing.[28] It was reported that porphyrin and its derivatives could be introduced into honeycomb films by acting as a fluorescent indicator,[29] the core of star polymers,[30] and a bactericide.[31,32] However, these breath figure films were generally fabricated from polystyrene-based polymers, which cannot be used at elevated temperature because of their low thermal stability. There is a critical demand for thermally stable breath figure films that can be used for chemical sensing at high temperature.

Aromatic polyimides[33] is a kind of thermally stable polymer and has been widely used for photoresists,[34] gas separation membranes,[35] electroluminescence devices,[36] and fuel cells materials.[37] We previously reported that porphyrin can be incorporated into aromatic polyimides by copolymerization and the porphyrinated polyimides (PPIs) were electrospun as nanofiber nonwoven mats to detect HCl and 2,4,6-trinitro-toluene trinitrotoluene (TNT) vapors.[38,39] However, the nonwoven structure is not stable and the nanofiber mats are not easy to be directly fabricated on the sensor surface.[40] Honeycomb films, on the other hand, are more stable than the nonwoven nanofibers and are also possible to be directly fabricated on the sensor surface. Herein, we report thermally stable honeycomb films by simply breath-figure method from these porphyrinated polyimides for HCl sensing. We investigated the effects of porphyrin content in the polyimides on the assembly behaviour during the breath figure process. A calculation of interaction between the porphyrin units and the water molecules was performed based on density functional theory (DFT) to further understand the formation of the ordered,

multilayered honeycomb porous films. HCl sensing property of the PPI honeycomb films was examined, and the results reveal that the honeycomb films show larger fluorescence quenching than that of the corresponding dense films. Moreover, the outstanding thermal stability of the PPI honeycomb films inherited from aromatic polyimide was demonstrated, which provides potential applications in the detection of gases (e.g., HCl) in harsh environment such as exhaust gas leaked from waste incinerators.

Experimental

Materials

All the chemicals were analytical reagents. 5,10-*Bis*(4-aminophenyl)-15,20-diphenyl-porphyrin (*cis*-DATPP) was synthesized according to the literature published by Luguya *et al.*[41] PPIs were synthesized by a one-step polymerization method from 4,4'-hexafluoro-isopropylidenediphthalic anhydride (6FDA), 4,4'-diaminodiphenyl ether (ODA), and *cis*-DATPP according to our previous work.[42] The synthetic route is shown in Scheme S1 in Electronic Supplementary Information, ESI. By controlling the addition amount of *cis*-DATPP, we synthesized PPIs with different porphyrin contents of 0, 4.93, 9.85, and 14.89 mol% relative to the total diamine monomers (ODA + *cis*-DATPP), which are noted as HPI, 5PPI, 10PPI, 15PPI, respectively. Poly(ethylene terephthalate) (PET) films were kindly provided by Hangzhou Tape Factory (China) and cleaned with acetone for 5 min and repeated three times before used.

Preparation of honeycomb films

The honeycomb films were casted by the typical breath figure method.[43] Polyimide was dissolved in chloroform to form a homogeneous solution with a concentration of 2 mg/mL. An aliquot of 50 μL for each honeycomb film was drop-cast onto a PET film or a quartz plate placed under a 2.0 L/min humid airflow (25 °C and >90% RH). The solution soon turned turbid, owing to the evaporation of chloroform. After solidification, the film was dried at room temperature. For comparison, a dense film was prepared from 15PPI in ambient condition in the absence of humid airflow.

Computational methods

DFT computations were carried out with Becke3LYP (B3LYP) hybrid density function using Gaussian 03 program package.[44] A 6-31+G (d, p) basis set was used for the geometry optimizations and energy calculations of model compounds. The interaction energy ($E_{interaction}$) was calculated between a porphyrin molecule and a water molecule from the equation below:

$$E_{interaction} = E_{complex} - (E_{porphyrin} + E_{water})$$

where $E_{complex}$, $E_{porphyrin}$, and E_{water} are energies of porphyrin-water complex, porphyrin molecule, and water molecule, respectively.

Thermal stability test of the honeycomb films

Honeycomb films for thermal stability test were fabricated on clean quartz plates, instead of PET films, by the breath figure method using the same procedure. The films were heated in a mufflefurnace at 200 °C, 300 °C, or 400 °C for 2 h. Surface morphology was observed to evaluate the thermal stability of the films.

Sensing performance of the honeycomb films to HCl gas

In the case of HCl gas detection, PPI honeycomb films were prepared on clean quartz plates. HCl vapor with a concentration of 100 ppm was acquired by controlling the concentration of HCl aqueous solution in a sealed testing chamber (500 mL) at 25 °C. After exposing to the HCl gas for designated time, sensing property of the PPI honeycomb films was determined by measuring the fluorescence intensity. After each measurement, the chamber was puffed with ammonia gas for 5 s and then with nitrogen gas three times for 3 min each to recover the honeycomb films.

Characterization

^{1}H NMR spectra were recorded on a Bruker (Advance Ⅲ 400) NMR instrument at room temperature with $CDCl_3$ as solvent. UV-visible and fluorescence spectra were determined on Shimadzu (UV-2450) and Shimadzu (RF-5301PC) spectrometer, respectively. Field emission scanning electron microscope (FESEM, FEI-SIRION-100) was used to observe the surface morphology of films. DSC/TGA analysis was recorded on the DSC Q1000 instrument for the synthetic polymers under nitrogen atmosphere with a heating rate of 5 °C/min. Fluorescence images were taken by Laser scanning confocal microscope (ZEISS LSM780 Germany) from the honeycomb films.

Results and discussion

Preparation and characterization of the honeycomb films

Honeycomb films were prepared from PPIs with different porphyrin contents (Figure S1) via a typical breath figure procedure. Homopolyimide (HPI) without porphyrin units, which was polymerized from 6FDA and ODA, was also fabricated into honeycomb film under the same condition. Figure 1 shows that the regularity of the honeycomb film changes little with the increase of porphyrin contents in the polyimides. It was reported that the morphology of honeycomb films is strongly influenced by polymer structures.[45] For example, polystyrene without any polar end groups is able to form honeycomb film under certain condition,[46] however, the film regularity can be significantly improved when polar blocks or end groups are incorporated into the polymers.[47-49] It is generally accepted that the condensed water droplets can be effectively stabilized and prevented from coalescing by the hydrophilic blocks or end groups of polymers in the breath figure process.[25,45,50] In this study, we suggest the porphyrin units are able to interact with the water molecules, which promotes the formation of ordered honeycomb films. This hypothesis will be further discussed on the basis of theoretical calculation in the following text.

Figure 2 summarizes the pore diameter and pore center distance of the honeycomb films by analyzing the top-down FESEM images. It can be seen that both pore diameter and pore center distance decrease gradually with the increase of porphyrin content in the polyimides. This results may support the hypothesis that the porphyrin units are able to interact with and to stabilize water droplets because a series of work[45-50] demonstrate that increasing the ability of polymer to stabilize water droplets can lead to not only high regularity but also small pore size for the honeycomb films.[15]

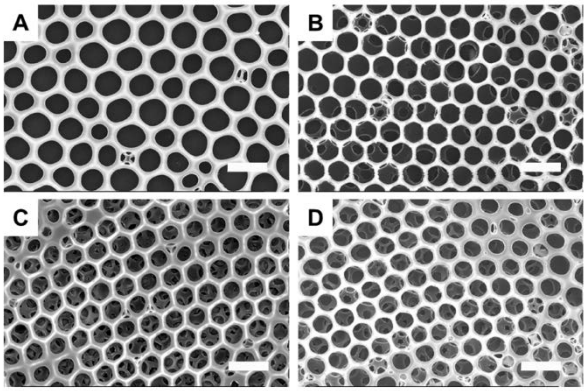

Figure 1. FESEM images of honeycomb films fabricated from (A) HPI, (B) 5PPI, (C) 10PPI, and (D) 15PPI. Scale bar is 2 μm.

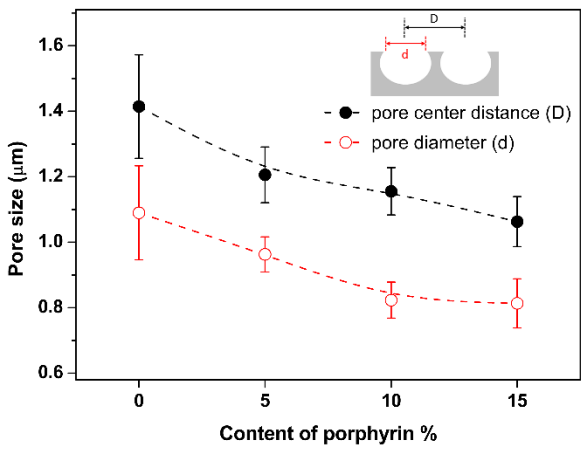

Figure 2. Correlation between pore diameter (d) and pore center distance (D) with the content of porphyrin in PPIs.

It is worth pointing out that PPI honeycomb films exhibit multilayer structure whereas the film prepared from HPI is monolayered (Figure 1). Similar phenomena have been reported for other polymers with different end groups or from different solutions.[51] Srinivasarao and co-workers suggested that the formation of multilayer structure is due to the fast sinking of condensed water droplets into polymer solution by Marangoni effect.[9] After sinking of the first layer, the following condensed water droplets continue to assemble into the solution to form the second layer. Then, a multilayer structured honeycomb film is generated through repeating the process above. Hao et al. proposed that the driving forces, the film thickness, and the solidification time are important factors for the formation of multilayer structure.[52] During the Marangoni convection, the driving force acting on water droplets depends on the interaction between polymer and water droplets. Therefore, polymers having strong interaction with water, for example, PPIs, will facilitate the formation of multilayer structure when other experimental conditions such as polymer concentration and casting thickness are the same.

Interaction of PPI with water

DFT was applied to calculate the interaction of water molecules with the studied PPIs for supporting the above-mentioned hypothesis. To simplify this calculation, 5,10,15,20-tetraphenylporphyrin (TPP), diphenyl ether, and *N*-methylphthalimide were used to represent porphyrin unit, ether group, and imide group in the PPIs, respectively. Figure 3 shows the optimized configurations of each model molecule interacting with a water molecule by geometry optimization. They were taken from the energy minimization by DFT calculation. It can be seen from Figure 3A and B that the water molecule locates on the center of porphyrin ring plane and the H-O bond points to the center of porphyrin near the four pyrrole N atoms. Figure 3C and D gives the optimized configurations of diphenyl ether and *N*-methylphthalimide interacting with a water molecule. They all display a specific alignment of interaction pairs between the H-O bond of water molecule and hydrogen bond acceptor of the model molecule. Such alignment is the characteristic of hydrogen bonds.

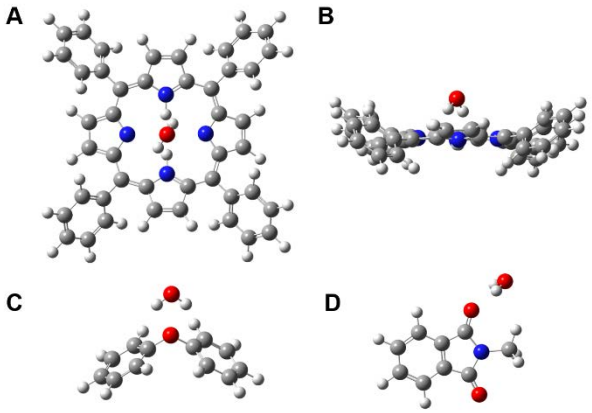

Figure 3. Optimized configurations for (A, B) TPP, (C) diphenyl ether, and (D) *N*-methylphthalimide interacting with a water molecule. Red, white, grey, and blue balls represent oxygen, hydrogen, carbon, and nitrogen atoms, respectively.

Table 1 summarizes the binding energies (ΔE) of the model molecules interacting with water molecules computed at DFT B3LYP/6-31+G (d, p) level. The binding energy of TPP and H_2O is 47.69 kJ/mol, which means that the interaction between the two molecules is almost twice stronger than that of hydrogen bond N···H-O, which has a binding energy of 29 kJ/mol.[53] The binding energy of *N*-methylphthalimide and H_2O is 26.05 kJ/mol, and that of diphenyl ether and H_2O is 23.77 kJ/mol. These values indicate both of the interactions are weaker than that between porphyrin and water. Therefore, it is obvious that the incorporation of porphyrin units into polyimide can increase the interaction of the polymer with water in the breath figure process. It is consistent with experimental results including the changes in pore diameter and the formation of multilayer structure mentioned above.

Table 1. Binding Energy (ΔE) Calculated by B3LYP/6-31+G (d, p) Level of Density Functional Theory

ΔE Hartree (kJ/mol)	H_2O
TPP	0.01816 (47.69)
diphenyl ether	0.009053 (23.77)
N-methylphthalimide	0.009923 (26.05)

Thermal stability of the honeycomb films

It is well known that aromatic polyimide is a kind of thermally

stable polymer.[54-57] As an example, 15PPI has a glass transition temperature (T_g) of 296 °C, and the temperature for 5% gravimetric loss is as high as 547 °C, which are very similar with those of aromatic polyimide (Figure S2 in ESI). In other words, the introduction of porphyrin units does not change the thermal stability of polyimide. This high glass transition temperature implies that the honeycomb films are stable when suffering from high temperature treatment. It can be seen from Figure 4 that the films retain the ordered three dimensional structures after heat treatment at 200 °C for 2 h. The pores remain without pore mergence after heating at 300 °C for 2 h, but they collapse to some extent. The ordered pore structure is destroyed when increasing the heating temperature to 400 °C. Overall, the PPI honeycomb films possess superior thermal stability compared with others such as those prepared from polystyrene, which makes the porphyrinated honeycomb films promising for high temperature sensing.

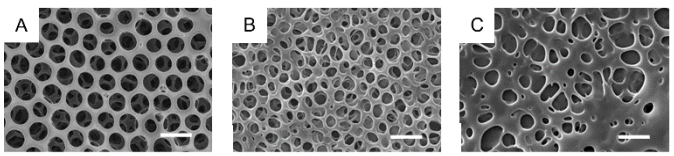

Figure 4. FESEM images of 15PPI honeycomb films treated at (A) 200 °C, (B) 300 °C, and (C) 400 °C for 2 h. Scale bar is 2 μm.

Sensing property of the honeycomb films to HCl gas

PPIs show a strong absorption peak at around 420 nm and a strong emission peak at 650 nm, which are similar with typical porphyrin (Figure S3 in ESI). They can be used for chemical sensing based on the photophysical properties of porphyrin, that is, fluorescence emission and quenching.[38,39] It is expected that the PPI honeycomb films have higher sensitivity than the corresponding dense film because the former has a porous structure. HCl gas was applied as the target analyte for the films pre-treated under different temperatures. CLSM was used to directly observe the emitted fluorescence from the honeycomb films as well as the dense film. Results confirm that all the honeycomb and dense films show red fluorescence before exposing to HCl gas (Figure 5A-D). The fluorescence is quickly quenched for the honeycomb films after exposing to HCl gas with a concentration of 100 ppm for 10 s (Figure 5E-G). These fluorescence changes are mainly attributed to the protonation of porphyrin moieties by HCl, and then the porphyrin rings change their conformation from planar to saddle structure. The distortion of porphyrin rings increase the energy resonance interaction of the phenyl groups with the porphyrin nucleus,[58-60] then fluorescence quenching can be observed obviously. Quenching ratio was employed to reflect the sensitivity to HCl gas, which was calculated by the value decrease and the initial value of fluorescence according Figure 5. The quenching ratio is about 79% for 15PPI honeycomb films at room temperature (Figure 6). It shows lower sensitivity than the PPI nanofibers reported in our former work,[38] which reaches 95%. This can be attributed to the three dimensional nonwoven structure and the high surface area of nanofibers. The quenching ratio slightly decreases with treatment temperature and remains higher than 72% for films treated even at 300 °C. This is due to the collapse of porous structures and then the accessibility decrease of HCl gas. However, it is only 50% for the corresponding dense film at room temperature. The significant fluorescence quenching of honeycomb films can be ascribed to their porous structures and hence good gas accessibility. Therefore, it can be concluded that the honeycomb films possess not only high sensitivity but also high-temperature sensing ability.

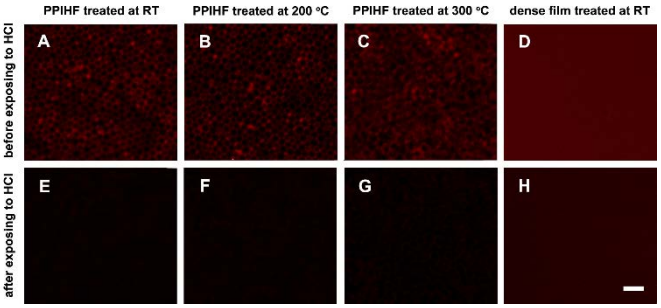

Figure 5. CLSM images of the 15PPI honeycomb films treated at different temperatures and the dense film before (top row, A-D) and after (bottom row, E-H) exposing to HCl gas. The excitation wavelength is 488 nm. Scale bar is 5 μm.

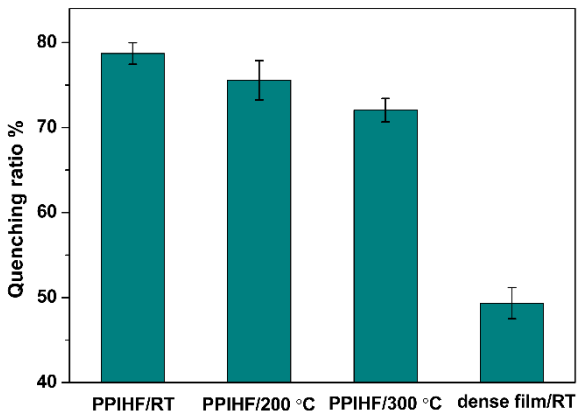

Figure 6. Fluorescence quenching ratio of the 15PPI honeycomb films treated at different temperatures and the dense films after exposing to HCl gas.

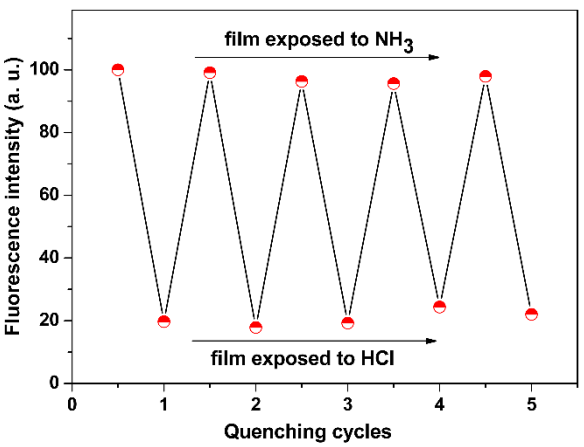

Figure 7. Regaining of the quenching efficiency for the 15PPI honeycomb film after exposing to HCl and NH_3 gases for five cycles.

The reusability of the honeycomb films was further measured by exposing to HCl gas and NH_3 gas alternately at room temperature. It can be seen that the green films turn back to red brown when exposing the quenched films to NH_3 gas for 5 s (Figure S4 in ESI). Changes in fluorescence intensity are shown in Figure 7. The initial emission intensity is almost fully recovered by simply exposing the films to NH_3 gas for 5 s. The quenching efficiency and regeneration property of the films remain nearly unchanged over five cycles of use, demonstrating reversible sensing ability, which was also observed from PPI dense films (Figure S5, in ESI).

Conclusion

We fabricated thermally stable honeycomb-patterned porous films for sensing of hazardous HCl gas. Porphyrinated polyimides with different porphyrin contents were synthesized and used for preparing the honeycomb films by the breath figure method. The films are ordered, and the pore diameters decrease with the porphyrin content. The honeycomb films prepared from porphyrinated polyimides have multilayered structure because the interaction between porphyrin unit and water molecule is stronger than those of ether group and imide group with water molecules. The porphyrinated honeycomb films possess high thermal stability and high sensitivity to HCl gas after treated at a wide temperature range from room temperature to 300 °C. Recovery experiments by ammonia gas also demonstrate the reusability of the honeycomb films. This work provides a novel chemical sensing material for monitoring HCl gas in incinerators from burning domestic, clinical or industrial wastes.

Acknowledgements

This work has been supported by the National Natural Science Foundation of China (Grant No. 21374100 and 50973094). We appreciate Mr. Liang-Wei Zhu and Mr. Yang Ou at the Department of Polymer Science and Engineering, Zhejiang University, for their experiment help and discussion.

Notes and references

[a]MOE Key Laboratory of Macromolecular Synthesis and Functionalization, Department of Polymer Science and Engineering, Zhejiang University, Hangzhou 310027, China. E-mail: lswan@zju.edu.cn (L.-S. Wan), xuzk@zju.edu.cn (Z.-K. Xu); Fax: +86 571 87951592

[b]Department of Chemistry, Zhejiang University, Hangzhou 310027, China. E-mail: jianwu@zju.edu.cn (J. Wu)

[c]Cyrus Tang Center for Sensor Materials and Applications, Zhejiang University, Hangzhou 310027, China

† Electronic Supplementary Information (ESI) available: See DOI: 10.1039/b 000000x/

1 X. J. Huang and Y. K. Choi, *Sens. Actuators, B*, 2007, **122**, 659-671.
2. L. Basabe-Desmonts, D. N. Reinhoudt and M. Crego-Calama, *Chem. Soc. Rev.*, 2007, **36**, 993-1017.
3. V. S.-Y. Lin, K. Motesharei, K.-P. S. Dancil, M. J. Sailor and M. R. Ghadiri, *Science*, 1997, **278**, 840-843.
4. L. Jia and W. Cai, *Adv. Func. Mater.*, 2010, **20**, 3765-3773.
5. T. J. Barton, L. M. Bull, W. G. Klemperer, D. A. Loy, B. McEnaney, M. Misono, P. A. Monson, G. Pez, G. W. Scherer, J. C. Vartuli and O. M. Yaghi, *Chem. Mater.*, 1999, **11**, 2633-2656.
6. M. E. Davis, *Nature*, 2002, **417**, 813-821.
7. D. Wu, F. Xu, B. Sun, R. Fu, H. He and K. Matyjaszewski, *Chem. Rev.*, 2012, **112**, 3959-4015.
8. G. Widawski, M. Rawiso and B. Francois, *Nature*, 1994, **369**, 387-389.
9. M. Srinivasarao, D. Collings, A. Philips and S. Patel, *Science*, 2001, **292**, 79-83.
10. H. M. Ma and J. C. Hao, *Chem. Soc. Rev.*, 2011, **40**, 5457-5471.
11. H. Bai, C. Du, A. Zhang and L. Li, *Angew. Chem. Int. Edit.*, 2013, **52**, 12240-12255.
12. L.-S. Wan, L.-W. Zhu, Y. Ou and Z.-K. Xu, *Chem. Commun.*, 2014, **50**, 4024-4039.
13. A. Munoz-Bonilla, M. Fernandez-Garcia and J. Rodriguez-Hernandez, *Prog. Polym. Sci.*, 2014, **39**, 510-554.
14. A. Boker, Y. Lin, K. Chiapperini, R. Horowitz, M. Thompson, V. Carreon, T. Xu, C. Abetz, H. Skaff, A. D. Dinsmore, T. Emrick and T. P. Russell, *Nat. Mater.*, 2004, **3**, 302-306.
15. Y. Fukuhira, H. Yabu, K. Ijiro and M. Shimomura, *Soft Matter*, 2009, **5**, 2037-2041.
16. X. L. Jiang, X. F. Zhou, Y. Zhang, T. Z. Zhang, Z. R. Guo and N. Gu, *Langmuir*, 2010, **26**, 2477-2483.
17. X. F. Li, L. A. Zhang, Y. X. Wang, X. L. Yang, N. Zhao, X. L. Zhang and J. Xu, *J. Am. Chem. Soc.*, 2011, **133**, 3736-3739.
18. Z. Zhang, T. C. Hughes, P. A. Gurr, A. Blencowe, X. Hao and G. G. Qiao, *Adv. Mater.*, 2012, **24**, 4327-4330.
19. L. S. Wan, Q. L. Li, P. C. Chen and Z. K. Xu, *Chem. Commun.*, 2012, **48**, 4417-4419.
20. L. P. Heng, X. F. Meng, B. Wang and L. Jiang, *Langmuir*, 2013, **29**, 9491-9498.
21. J. Li, Y. Li, C. Y. K. Chan, R. T. K. Kwok, H. Li, P. Zrazhevskiy, X. Gao, J. Z. Sun, A. Qin and B. Z. Tang, *Angew. Chem.-Int. Edit.*, 2014, **53**, 13518-13522.
22. Y. Ou, C. J. Lv, W. Yu, Z. W. Mao, L. S. Wan and Z. K. Xu, *ACS Appl. Mater. Interfaces*, 2014, **6**, 2400-22407.
23. W. Wang, C. Du, X. Wang, X. He, J. Lin, L. Li and S. Lin, *Angew. Chem.-Int. Edit.*, 2014, **53**, 12116-12119.
24. B. B. Ke, L. S. Wan and Z. K. Xu, *Langmuir*, 2010, **26**, 8946-8952.
25. P.-C. Chen, L.-S. Wan, B.-B. Ke and Z.-K. Xu, *Langmuir*, 2011, **27**, 12597-12605.
26. X. C. Sun, C. Bruckner, M. P. Nieh and Y. Lei, *J. Mater. Chem. A*, 2014, **2**, 14613-14621.
27. Y. Ou, L. Y. Wang, L. W. Zhu, L. S. Wan and Z. K. Xu, *J. Phys. Chem. C*, 2014, **118**, 11478-11484.
28. W.-S. Li and T. Aida, *Chem. Rev.*, 2009, **109**, 6047-6076.
29. D. Fan, X. Xia, H. Ma, B. Du and Q. Wei, *J. Colloid and Interface Sci.*, 2013, **402**, 146-150.
30. L.-W. Zhu, L.-S. Wan, J. Jin and Z.-K. Xu, *J. Phys. Chem. C*, 2013, **117**, 6185-6194.
31. X. Y. Zhou, Z. H. Chen, Y. Z. Wang, Y. Guo, C. H. Tung, F. S. Zhang and X. W. Liu, *Chem. Commun.*, 2013, **49**, 10614-10616.
32. Y. Wang, Y. Liu, G. Li and J. Hao, *Langmuir*, 2014, **30**, 6419-6426.
33. D. J. Liaw, K. L. Wang, Y. C. Huang, K. R. Lee, J. Y. Lai and C. S. Ha, *Prog. Polym. Sci.*, 2012, **37**, 907-974.
34. M. S. Jung, W. J. Joo, B. K. Choi and H. T. Jung, *Polymer*, 2006, **47**, 6652-6658.
35. S. H. Huang, C. C. Hu, K. R. Lee, D. J. Liaw and J. Y. Lai, *Eur. Polym. J.*, 2006, **42**, 140-148.
36. Y. Kim, K. H. Bae, Y. Y. Jeong, D. K. Choi and C. S. Ha, *Chem. Mater.*, 2004, **16**, 5051-5057.
37. N. Asano, M. Aoki, S. Suzuki, K. Miyatake, H. Uchida and M. Watanabe, *J. Am. Chem. Soc.*, 2006, **128**, 1762-1769.
38. Y.-Y. Lv, J. Wu and Z.-K. Xu, *Sens. Actuators, B*, 2010, **148**, 233-239.
39. Y.-Y. Lv, W. Xu, F.-W. Lin, J. Wu and Z.-K. Xu, *Sens. Actuators, B*, 2013, **184**, 205-211.
40. Z.-G. Wang, Y. Wang, H. Xu, G. Li, Z.-K. Xu, *J. Phys. Chem. C*, 2009, **113**, 2955-2960.
41. R. Luguya, L. Jaquinod, F. R. Fronczek, M. G. H. Vicente and K. M. Smith, *Tetrahedron*, 2004, **60**, 2757-2763.
42. Y.-Y. Lv, J. Wu, L.-S. Wan and Z.-K. Xu, *J. Phys. Chem. C*, 2008, **112**, 10609-10615.
43. L. S. Wan, B. B. Ke, J. Zhang and Z. K. Xu, *J. Phys. Chem. B*, 2012, **116**, 40-47.
44. Q.-Y. Wu, X.-N. Chen, L.-S. Wan and Z.-K. Xu, *J. Phys. Chem. B*, 2012, **116**, 8321-8330.
45. M. H. Stenzel, C. Barner-Kowollik and T. P. Davis, *J. Polym. Sci., Part A: Polym. Chem.*, 2006, **44**, 2363-2375.

46. J. Peng, Y. C. Han, Y. M. Yang and B. Y. Li, *Polymer*, 2004, **45**, 447-452.
47. L. W. Zhu, W. Yang, L. S. Wan and Z. K. Xu, *Polym. Chem.*, 2014, **5**, 5175-5182.
48. L. W. Zhu, B. H. Wu, L. S. Wan and Z. K. Xu, *Polym. Chem.*, 2014, **5**, 4311-4320.
49. L. W. Zhu, Y. Ou, L. S. Wan and Z. K. Xu, *J. Phys. Chem. B*, 2014, **118**, 845-854.
50. U. H. F. Bunz, *Adv. Mater.*, 2006, **18**, 973-989.
51. L. W. Zhu, W. Yang, Y. Ou, L. S. Wan and Z. K. Xu, *Polym. Chem.*, 2014, **5**, 3666-3672.
52. R. Dong, J. Yan, H. Ma, Y. Fang and J. Hao, *Langmuir*, 2011, **27**, 9052-9056.
53. D. Sitkoff, K. A. Sharp and B. Honig, *J. Phys. Chem.*, 1994, **98**, 1978-1988.
54. H. Yabu, M. Tanaka, K. Ijiro and M. Shimomura, *Langmuir*, 2003, **19**, 6297-6300.
55. Y. Tian, S. Liu, H. Ding, L. Wang, B. Liu and Y. Shi, *Polymer*, 2007, **48**, 2338-2344.
56. L. Wang, Y. Tian, H. Ding and B. Liu, *Eur. Polym. J.*, 2007, **43**, 862-869.
57. X. Xu, L. Heng, X. Zhao, J. Ma, L. Lin and L. Jiang, *J. Mater. Chem.*, 2012, **22**, 10883-10888.
58. A. Stone, E. B. Fleischer, *J. Am. Chem. Soc.*, 1968, **90**, 2735-2748.
59. V. N. Knyukshto, K. N. Solovyov, A. F. Mironov, G. D. Egorova, A. V. Efimov, *Opt. Spectrosc.*, 1998, **85**, 540-547.
60. V. N. Knyukshto, K. N. Solovyov, G. D. Egorova, *Biospectroscopy*, 1998, **4**, 121-133.

Table of Contents Graphic

Manuscript: Porphyrinated Polyimide Honeycomb Films with High Thermal Stability for HCl Gas Sensing

Authors: Fu-Wen Lin, Xiao-Ling Xu, Ling-Shu Wan*, Jian Wu, and Zhi-Kang Xu*

Thermally stable films with ordered pores are fabricated from porphyrinated polyimides and they exhibit excellent property in HCl gas sensing.